論文 / 著書情報
Article / Book Information

論題(和文)	
Title(English)	MULTI-MEGACITY INVESTIGATION OF HEAT WAVE EVENTS UNDER VARIOUS CLIMATE CHANGE AND URBANIZATION SCENARIOS
著者(和文)	DO KHANH NGOC, Varquez Alvin Christopher Galang, 神田 学
Authors(English)	Do Ngoc KHANH, Alvin C. G. VARQUEZ, Manabu KANDA
出典(和文)	, Volume 12, Issue 2,
Citation(English)	Journal of JSCE, Volume 12, Issue 2,
発行日 / Pub. date	2023, 9
権利情報 / Copyright	本著作物の著作権は土木学会に帰属します。 Copyright (c) 2023 Japan Society of Civil Engineers.

MULTI-MEGACITY INVESTIGATION OF HEAT WAVE EVENTS UNDER VARIOUS CLIMATE CHANGE AND URBANIZATION SCENARIOS

Do Ngoc KHANH[1], Alvin C. G. VARQUEZ[2] and Manabu KANDA[3]

[1]Student Member of JSCE, Dept. of Transdisciplinary Sci. and Eng., Tokyo Institute of Technology
(2-12-1 Ookayama, Meguro-ku, Tokyo, 152-8550, Japan)
E-mail: do.k.aa@m.titech.ac.jp (Corresponding Author)
[2]Member of JSCE, Associate Professor, Dept. of Transdisciplinary Sci. and Eng., Tokyo Institute of Technology
(2-12-1 Ookayama, Meguro-ku, Tokyo, 152-8550, Japan)
E-mail: varquez.a.aa@m.titech.ac.jp
[3]Member of JSCE, Professor, Dept. of Transdisciplinary Sci. and Eng., Tokyo Institute of Technology
(2-12-1 Ookayama, Meguro-ku, Tokyo, 152-8550, Japan)
E-mail: kanda.m.aa@m.titech.ac.jp

In 2022, intense heat waves occur all around the world. In this study, we project these heat waves into the future with futuristic projection of hourly varying spatially distributed anthropogenic heat for three megacities—Delhi, London, and Tokyo. Different future climate forcing (CMIP5 and CMIP6) was also compared. We found that if similar heat waves occur in the future, they may be 0.8 to 1.5 °C hotter than the past events, on average. Urbanization in Delhi may severely worsen the heat wave, while projected decrease in energy usage in London and Tokyo may make the heat waves less severe. For the concerned heat wave events, urbanization effect was also found to be stronger in nighttime than daytime and exhibits large spatial heterogeneity and dependence on background climate forcing. Difference between CMIP5 and CMIP6 was significant but was much less than the difference between CMIP5/CMIP6 and the present.

Key Words: *climate change, urbanization, heat wave, CMIP.*

1. INTRODUCTION

In 2022, intense heat waves occur all around the world. Temperature surpassed 40 °C, broke records in many places, severely affected human health, infrastructures, and economic activities[1)]. Previous research revealed that urban area are affected more severely by heat waves than rural areas[2)]. As climate change progresses, it has been projected that in the future, heat waves might occur more frequently[3)]. Projection at global, regional scale[4)] and projection for individual cities[5)] have been done. However, there is currently a lack of studies covering many cities worldwide with diverse background and lack of consideration of futuristic urbanization projection (e.g., projection of change in anthropogenic heat driven by socioeconomic scenarios). For that reason, in this study, we attempt to project three heat waves events occurred in 2022 in three megacities—Delhi (India), London (UK), and Tokyo (Japan)—to the future (the 2050s) using two different sets of global climate projection (the older Coupled Model Intercomparison Project Phase 5 (CMIP5) and the newer CMIP6), together with futuristic projection of urbanization of the three cities under the worst case scenario (SSP3 coupled with RCP8.5). Our targets are:

- projecting the general characteristics of the heat wave events if they reoccur in the future,
- quantifying the contribution of urbanization,
- quantifying the significance of the choice global climate projections (i.e., CMIP5 vs CMIP6).

2. METHODOLOGY

A modified version of the Weather Research and Forecast (WRF) model that can considered spatially varying urban morphological parameters and spatiotemporally varying anthropogenic heat was used[6)]. Simulation were

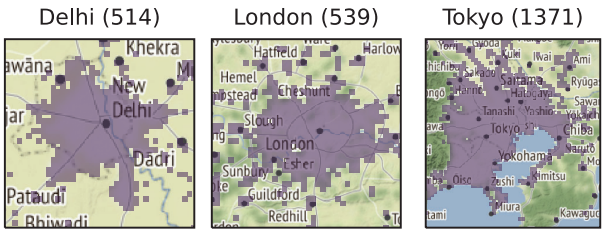

Fig. 1 Analysis domains (a part of domain 2). The number in the brackets following each city name is the number of urban grids (purple shaded).

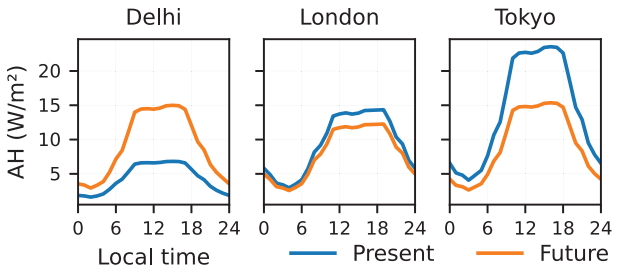

Fig. 2 Comparison between spatial average of hourly anthropogenic heat between the present and the future.

conducted for Tokyo (2022/06/24–2022/07/02), Delhi (2022/04/06–2022/04/11) and London (2022/07/17–2022/07/19) with the first simulation days used for model spin-up and were excluded from all analysis. Model configuration is described below.

Each city was simulated using two domains with one-way nesting: 10 km resolution (101-by-101 grids) and 2 km resolution (101-by-101 grids for Delhi and London and 151-by-151 grids for Tokyo). The two domains are concentric and centered at 28.6° N 77.1° E, 51.5° N 0.2° W, and 35.5° N 140.0° E for Delhi, London, and Tokyo, respectively (see also **Fig. 1**).

The ERA5 reanalysis dataset (hourly temporal resolution, 0.25° spatial resolution) was supplied as initial and boundary conditions to the model for the present climate forcing cases. Pseudo-global warming (PGW) method[7] was applied for the future climate forcing cases. Specifically, GCM outputs of five variables (surface temperature and vertical profiles of two wind velocity components, air temperature, and geopotential height). were extracted for the target month in the 2015–2024 decade and the 2046–2055 decade from the CMIP5 and CMIP6 database. For each variable, the difference between its temporal and ensemble averages over the two decades were added to the aforementioned ERA5 reanalysis dataset to create the initial and boundary conditions for the cases with future climate forcing. For cases with CMIP5 forcing, five GCM members (rcp8.5 runs of GFDL-ESM2M, HadGEM2-ES, IPSL-CM5A-LR, MIROC-ESM-CHEM, NorESM1-M) were used. For cases with CMIP6 forcing, five GCM members (ssp5-8.5 runs of GFDL-ESM4, HadGEM3-GC31-MM, IPSL-CM6A-LR, MIROC6, NorESM2-MM) were used. For all GCM members, only the most commonly available ensemble is used (i.e., r1i1p1 for CMIP5 and r1i1p1f1 for CMIP6 except HadGEM3-GC31-MM for which r1i1p1f3 is used because r1i1p1f1 is not available for the necessary variables). Even though the CMIP5 members and the CMIP6 members are not exactly the same, they are of the same family and the CMIP6 members are newer version of the CMIP5 members.

Table 1 Simulation scenarios. Each scenario name has two characters: the first character represent climate forcing (P, 5, and 6 for present, CMIP5, and CMIP6, respectively), and the second character represent urbanization (P and F for present and future, respectively).

Scenario	Climate forcing	Urbanization
PP	Present	Present
PF	Present	Future
5P	CMIP5	Present
5F	CMIP5	Future
6P	CMIP6	Present
6F	CMIP6	Future

Here, we note that in CMIP6, there are two scenarios SSP3-7.0 and SSP5-8.5 (SSP3-8.5 does not exist in CMIP6). However, our urban morphological dataset and anthropogenic heat dataset (described later) were constructed under SSP3 and RCP8.5 assumptions of CMIP5. Therefore, for the cases with CMIP6 forcing, when choosing GCMs, we prioritize the match of radiative forcing (RCP8.5) over the match of socioeconomic pathways (SSP5 and SSP3). We note that GCMs' humidity output was not used to modify the boundary condition manually because of weak global surface relative humidity trend[8] and improper treatment of humidity information may lead to over-saturated atmosphere[9].

Spatially varying urban morphological parameters were estimated from population, nighttime lights, and gross domestic product (GDP) as in a previous study[6]. The AH4GUC present and future global 1 km hourly anthropogenic heat dataset[10] was also inputted to the model (**Fig. 2**). We note that the AH4GUC dataset was generated for the 2010s and 2050s decade under assumption of CMIP5 instead of the newer CMIP6. However, we use this dataset in this study because at the moment, there is no equivalent dataset under the assumption of CMIP6. Two urbanization scenarios were considered (present and future). The difference between the two scenarios is only in the change of anthropogenic heat. We did not change the urban morphological parameters between the present and the future cases. Similar to a previous research[6], we mod-

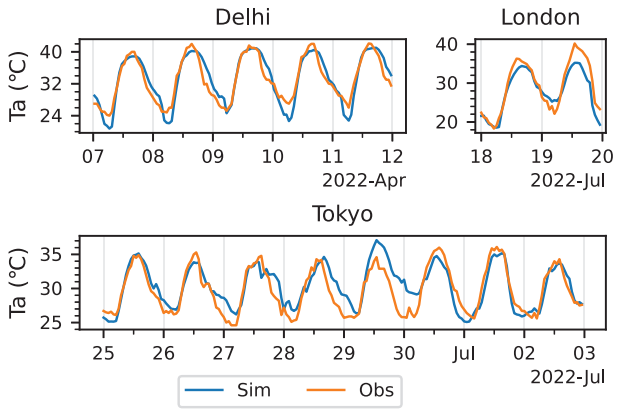

Fig. 3 Comparison between observed air temperature (orange lines) and simulated near surface air temperature (blue lines).

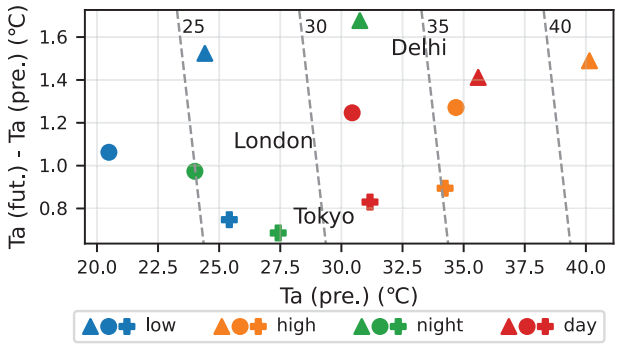

Fig. 4 Comparison between present (scenario PP) and projected future (scenario 6F) average daily low/high temperature and nighttime/daytime mean air temperature over the heat wave periods for Delhi, London, and Tokyo. Slanting dashed lines connect points with equal sum of x- and y-axis, which can be used to read projected future temperature.

ified the MODIS land use dataset included in the WRF model package by setting all grids with population count of at least 1000 to urban category. The same land use dataset is used for all simulations (i.e., no future land use projection is considered).

With three climate forcing scenarios (present, future under CMIP5, future under CMIP6) and two urbanization scenarios (present, future), six simulations were conducted for each cities as in **Table 1**.

3. RESULTS AND DISCUSSION

(1) Model verification

Simulation results (scenario PP) were verified against observation data downloaded from the NOAA Integrated Surface Database (ISD) (Indira Gandhi International Airport station for Delhi, Heathrow station for London, and Tokyo station for Tokyo). Comparison between hourly observed air temperature and near surface hourly simulated air temperature (air temperature at the first level of WRF model; hereinafter, air temperature) is shown in **Fig. 3**. Even though observation data was point observation and simulation data is 2 km by 2 km grid value, it can be seen that the the model capture well diurnal variation and peaks. The Pearson correlation coefficient is 0.93, 0.95, and 0.86, root mean square error is 2.22, 2.58, and 1.81 °C, respectively for Delhi, London, and Tokyo. In this study, we mainly focus on the difference between simulation cases, thus, it is expected model bias will be minimized by subtraction. To get a reliable projection of future temperature (in terms of actual value, not increment), bias correction is necessary; however, it is not in the scope of this study. From the above analysis, we conclude that the model has adequate performance to study the concerned heat wave events.

(2) Overall projection

In this section, we give an overall projection of the heat wave events into the future by comparing scenario PP and scenario 6F. In **Fig. 4**, we compare the present and projected future average daily low/high temperature and nighttime/daytime mean temperature over the heat wave periods for the three cities. We found that if similar heat wave events happen in the future, all temperature indices will be higher than the present by 0.8, 1.1, and 1.5 °C on average in Tokyo, London, and Delhi, respectively.

(3) Effects of urbanization

Under the simulation configuration of this study, the effect of urbanization (i.e., changing anthropogenic heat) can be estimated in three different ways by comparing scenario PP with PF, 5P with 5F, or 6P with 6F. Let the urbanization effect extracted by those comparison be UP, U5, and U6, respectively. By comparing UP, U5, and U6 together, we can judge whether or not the effect of urbanization is influenced by background climate conditions. Specifically, if UP, U5, and U6 are all equals to each other, we can conclude that urbanization effect is independent from background climate conditions. On the contrary, if the three differs, there is a mechanism that suppresses or enhances urbanization effect. In this study, we focus specifically on air temperature change at urban areas (i.e., grids classified as urban in the model, see **Fig. 1**). We will first discuss general characteristics of the effect and then discuss the interaction between urbanization and background climate.

a) General characteristics of urbanization effect

Time average of urbanization effect (UP, U5, and U6) over the heat wave periods at each urban grid was calculated. The spatial distribution of the time average is shown in **Fig. 5** in the form of kernel density

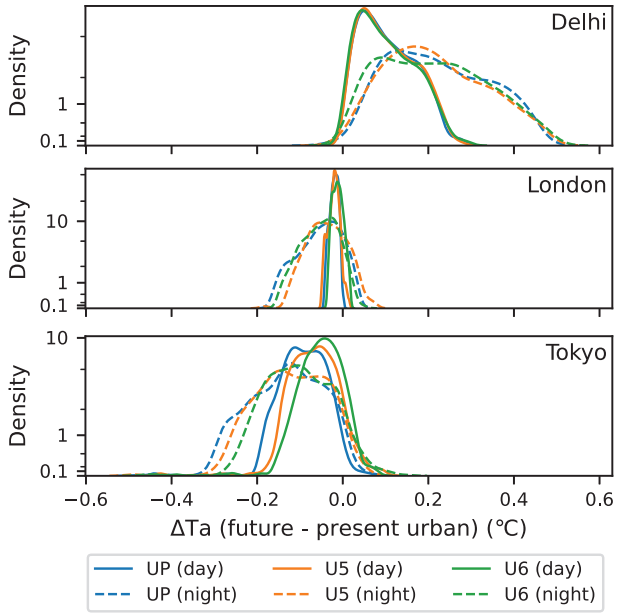

Fig. 5 Comparison between urbanization effects evaluated under different background climate conditions in daytime (solid lines) and nighttime (dashed lines). The lines represent the spatial distribution (kernel density estimation) of time average of urbanization effect at each urban grid over the heat wave periods.

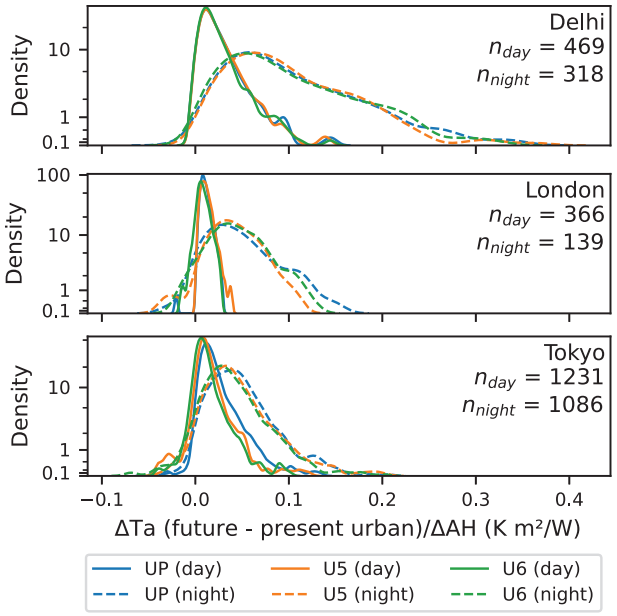

Fig. 6 Similar to **Fig. 5** but the average daytime/nighttime temperature change at each grid is normalized by the average daytime/nighttime anthropogenic heat change at that grid. Normalization is only done for grids with $|\Delta AH| \geq 1\ \mathrm{W/m^2}$. The number of grids satisfying the criterion is noted as n_{day} and n_{night}.

Table 2 Ensemble-spatial average and standard deviation of urbanization effect daytime and nighttime. Unit: 10^{-2} °C.

	Daytime		Nighttime	
	Mean	SD	Mean	SD
Delhi	9.3	5.6	21.0	10.5
London	-1.7	0.7	-4.5	2.9
Tokyo	-6.9	3.8	-11.6	6.9

estimation, separately for daytime and nighttime. In addition, spatial map of the time average of the UP, U5, and U6 ensemble was taken. The spatial average and standard deviation of that map for each city is shown in **Table 2**. The number of urban grids in each city is shown in **Fig. 1**. Overall, urbanization effect in Tokyo and London are negative because of projected decline in anthropogenic heat due to declining population; the reverse is true for Delhi, where population and anthropogenic heat are both projected to be increasing.

From **Fig. 5** and **Table 2**, it can be seen that in all three cities, the urbanization effect has larger mean (in terms of absolute value) and variance in nighttime than in daytime. Among the three cities, the mean value of urbanization effect is largest in Delhi at nighttime (0.21 °C), which is significant in the total warming at nighttime of 1.68 °C (**Fig. 4**). Depending on the location, the magnitude of urbanization effect is between −0.5 and 0.5 °C, with larger magnitude found in nighttime. This finding reaffirms findings from previous research[6),11)] that urbanization effect has large spatial variance. We note that while the previous research considered changes in both anthropogenic heat and urban morphological parameters, this study only considers the first factor.

To better explain the effect of anthropogenic heat, we normalize the average daytime/nighttime temperature change at each grid by the average daytime/nighttime anthropogenic heat change at that grid and plotted it in **Fig. 6**, which describes how much temperature changes per unit of anthropogenic heat. Note that normalization is only done for grids with change in anthropogenic heat of at least $1\ \mathrm{W/m^2}$ to avoid unwanted amplification of sensitivity due to division by near-zero value. The purpose of normalization is to investigate sensitivity of air temperature to anthropogenic heat, a linear relation between the two quantities is not implied. Similar to the analysis of pre-normalized temperature change (**Fig. 5**), it can be seen that urbanization effect is stronger and more heterogeneous in nighttime than in daytime. This can be explained by the fact that during daytime, stronger near surface wind and higher boundary layer allows anthropogenic heat to disperse both horizontally and vertically, making both absolute magnitude and variance of urbanization effect smaller than during nighttime. It can be seen in **Fig. 6** that the distributions at nighttime has long right tail. We inspected two-dimensional maps (not shown) of sensitivity visually and found that grids with high sensitivity tends to be in relatively less densely populated

Table 3 Difference between the means of UP, U5, and U6 at daytime and nighttime. Unit: 10^{-2} °C. Statistical significant derived from the Kolmogorov-Smirnov test is indicated by * ($p < 0.05$) and ** ($p < 0.01$).

		U5 - UP	U6 - UP	U6 - U5
Day	Delhi	0.0	-0.3	-0.3
	London	-0.1	0.6**	0.7**
	Tokyo	2.3**	4.1**	1.8**
Night	Delhi	-0.5	-0.7**	-0.2**
	London	0.9**	-0.2**	-1.1**
	Tokyo	1.0**	2.3**	1.3**

areas. One possible hypothesis for this phenomenon is that these areas have less buildings, thus, have smaller heat capacity, consequently, become more sensitive to anthropogenic heat. This hypothesis can be tested in future research by long term simulation of real atmospheric conditions or ideal simulations. It should be note that because anthropogenic heat is advected by wind and interacts with other components of the atmosphere, change in one location might be due to not only local anthropogenic heat change but also due to city-scale anthropogenic heat change and other factors. Therefore, this sensitivity analysis should be interpreted with care.

b) Urbanization–background climate interaction

As shown in **Fig. 5**, UP, U5, and U6 have similar distributions in daytime and similar distributions in in nighttime; however, the distributions do not completely overlap. In this section, we check whether or not the difference in the distributions are statistically significant. We use the Kolmogorov-Smirnov test for goodness of fit to test if the distributions of urbanization effect are identical. The result is summarized in **Table 3**. There are statistical evidence that the effect of urbanization is not independent from background climate forcing except for Delhi in daytime. The difference between the means of UP, U5, and U6 are in the order of 10^{-3} to 10^{-2} °C. Comparing the difference between the means (in **Table 3**) to the means (in **Table 2**) for Tokyo and London (daytime and nighttime), we found that the maximum difference is 20 to 59 % of the corresponding means in terms of magnitude, therefore, nonnegligible. However, the difference between the means is about two orders of magnitude smaller than the means for Delhi. This finding suggests that the effect of changing anthropogenic heat varies significantly with background climate for Tokyo and London, but negligible for Delhi, for the concerned heat wave events. We note that the dependency/independency discussed here is limited to the context of the analyzed heat wave events.

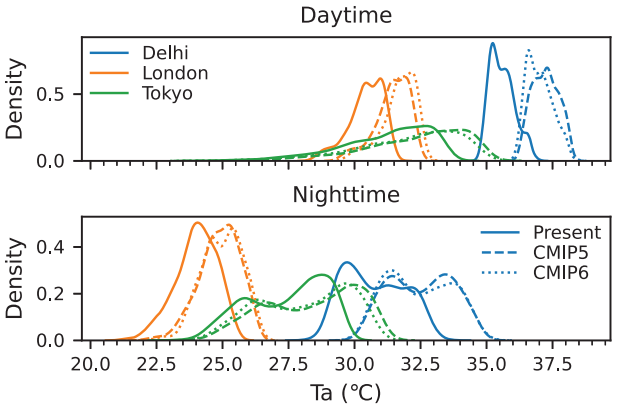

Fig. 7 Spatial distribution of average daytime/nighttime temperature over the heat wave events in the present (scenario PP), under CMIP5 forcing (scenario 5F), and under CMIP6 forcing (scenario 6F).

(4) Future climate forcing: CMIP5 and CMIP6

Next we examine if the choice of climate forcing (CMIP5 or CMIP6) has significant influence on the projected future heat wave events. We compare the spatial distribution of average daytime/nighttime temperature over the heat wave events under present (scenario PP), CMIP5 (scenario 5F), and CMIP6 forcing (scenario 6F) for the three cities. The result is shown in **Fig. 7**.

Similar to the investigation of urbanization effect, we conducted the Kolmogorov-Smirnov statistical test to check if the temperature distribution under CMIP5 and CMIP6 forcing are identical. We found that the difference between CMIP5 and CMIP6 was statistically significant for all cities in daytime and for Tokyo in nighttime ($p < 0.01$), and insignificant for Delhi and London at nighttime ($p \geq 0.05$). In the statistical significant cases, the mean difference between CMIP5 and CMIP6 was (in absolute magnitude) between 0.22 and 0.31 °C. One hypothesis for this difference is that numerical models (GCMs) have been updated. Moreover, CMIP5 was based on Representative Concentration Pathways (RCP, for example, RCP8.5) while CMIP6 was based on Shared Socioeconomic Pathways (SSP) coupled with radiative forcing (for example, SSP3-8.5). Therefore, it can be expected that CMIP5 and CMIP6 future projections are different as previous research has also pointed out[12].

While the choice of CMIP5 or CMIP6 has statically significant influence on the projected future heat wave events, it can be seen clearly from **Fig. 7** that the difference between CMIP5 and CMIP6 is much less than the difference between CMIP5/CMIP6 and the present. Moreover, we note that the minimum between CMIP5 and CMIP6 indicates that if these heat wave events repeat in the future, air temperature will be 1.41, 0.99 and 0.83 °C hotter in daytime and 1.68, 0.88 and 0.69 °C hotter in nighttime for Delhi, London, and Tokyo re-

spectively, on average. In other words, heat waves in the future is projected to be much hotter than in present, regardless of the choice of the older CMIP5 forcing or the newer CMIP6 forcing.

4. CONCLUSION

In this study, we attempted to project three heat waves event occurred in 2022 in three megacities—Delhi (India), London (UK), and Tokyo (Japan)—into the future (the 2050s) with consideration of different global climate forcing (CMIP5 and CMIP6) and futuristic projection of urbanization driven on socioeconomic changes under the worst-case scenario (SSP3 coupled with RCP8.5). The main findings are

1. Similar future heat waves will be approximately 0.8 to 1.5 °C hotter than the present. Average through the heat wave period, spatial mean of daily maximum temperature may reach 42, 36, and 35 °C (no bias correction) in Delhi, London, and Tokyo, respectively.
2. Urbanization (i.e., anthropogenic heat change) have stronger impact on the heat waves in nighttime than in daytime. In Delhi, urbanization may add 0.21 °C to nighttime temperature, on average. On the other hand, decreasing energy usage due to population decline in London and Tokyo may cool nighttime temperature down by 0.05 and 0.12 °C, on average, respectively.
3. Urbanization effect has large spatial variance. Absolute magnitude at certain locations in the cities may reach 0.50 °C.
4. Urbanization effect varies (statistically significantly) between different background climate (present, CMIP5, CMIP6), suggesting the existence of complex interaction between background climate condition and anthropogenic heat.
5. The choice of CMIP5 or CMIP6 as future climate forcing has statistically significant impact on the projection. However, the difference between CMIP5 and CMIP6 is much less significant than the difference between CMIP5/CMIP6 and the present.

There are several limitations of our work which can be addressed in future work such as: construction of anthropogenic heat and urban morphological parameters following CMIP6 assumptions and scenarios, evaluating the impact of not only anthropogenic heat change but also urban morphological parameters change. Moreover, in this study, we use an anthropogenic heat map for the average weather condition; however, under heat wave condition, anthropogenic heat might be much larger due to intensive usage of air conditioners. Future research might also address this shortcoming. Finally, to generalize the initial investigation results of this case-study, long-term and/or ideal simulation needs to be conducted.

ACKNOWLEDGMENT This work was supported by JSPS KAKENHI Grant Numbers JP21H04573, JP21K14249.

REFERENCES

1) NASA Earth Observatory. (2022). *Heatwaves and fires scorch Europe, Africa, and Asia*. Retrieved May 28, 2023, from https://earthobservatory.nasa.gov/images/150083/heatwaves-and-fires-scorch-europe-africa-and-asia
2) Li, D., & Bou-Zeid, E. (2013). Synergistic interactions between urban heat islands and heat waves: The impact in cities is larger than the sum of its parts. *J. Appl. Meteorol. Clim.*, *52*(9), 2051–2064. https://doi.org/10.1175/JAMC-D-13-02.1
3) Lhotka, O., Kyselỳ, J., & Farda, A. (2018). Climate change scenarios of heat waves in Central Europe and their uncertainties. *Theor. Appl. Climatol.*, *131*(3), 1043–1054. https://doi.org/10.1007/s00704-016-2031-3
4) Perkins-Kirkpatrick, S., & Gibson, P. (2017). Changes in regional heatwave characteristics as a function of increasing global temperature. *Sci. Rep.*, *7*(1), 1–12. https://doi.org/10.1038/s41598-017-12520-2
5) Lemonsu, A., Beaulant, A. L., Somot, S., & Masson, V. (2014). Evolution of heat wave occurrence over the Paris basin (France) in the 21st century. *Clim. Res.*, *61*(1), 75–91. https://doi.org/10.3354/cr01235
6) Khanh, D. N., Varquez, A. C. G., & Kanda, M. (2023). Impact of urbanization on exposure to extreme warming in megacities. *Heliyon*, *9*(4), e1551. https://doi.org/10.1016/j.heliyon.2023.e15511
7) Kimura, F., & Kitoh, A. (2007). Downscaling by pseudo global warming method. *The Final Report of ICCAP*, *4346*.
8) Dai, A. (2006). Recent climatology, variability, and trends in global surface humidity. *J. Clim.*, *19*(15), 3589–3606. https://doi.org/10.1175/JCLI3816.1
9) Brogli, R., Heim, C., Mensch, J., Sørland, S. L., & Schär, C. (2023). The pseudo-global-warming (PGW) approach: Methodology, software package PGW4ERA5 v1.1, validation, and sensitivity analyses. *Geosci. Model. Dev.*, *16*(3), 907–926. https://doi.org/10.5194/gmd-16-907-2023
10) Varquez, A. C. G., Kiyomoto, S., Khanh, D. N., & Kanda, M. (2021). Global 1-km present and future hourly anthropogenic heat flux. *Sci. Data*, *8*, 64. https://doi.org/10.1038/s41597-021-00850-w
11) Darmanto, N. S., Varquez, A. C. G., Kawano, N., & Kanda, M. (2019). Future urban climate projection in a tropical megacity based on global climate change and local urbanization scenarios. *Urban Clim.*, *29*, 100482. https://doi.org/10.1016/j.uclim.2019.100482
12) Hamed, M. M., Nashwan, M. S., & Shahid, S. (2022). Intercomparison of historical simulation and future projections of rainfall and temperature by CMIP5 and CMIP6 GCMs over Egypt. *Int. J. Clim.*, *42*(8), 4316–4332. https://doi.org/10.1002/joc.7468

(Received May 31, 2023)
(Accepted September 12, 2023)